Chapter 4

Collective and single particle behaviour of finite dust clusters under a transverse external magnetic field

The work included in this chapter is published in "H. Sarma and N. Das, Phys. Plasmas 31, 063704 (2024)".

The dynamics of two-dimensional dust clusters in plasma environment are studied at different strengths of a transverse external magnetic field, via Langevin dynamics simulation. The collective oscillation spectra obtained from simulation are compared with the dispersion relation derived from analytical calculation under harmonic approximation. At high magnetic field strength, in the case of a linear chain, a longitudinal optic branch emerges whereas in the case of a 2D isotropic cluster, two clear distinct branches appear with the high frequency branch approaching cyclotron frequency. Mean squared displacement is obtained for the 2D cluster as a probe of single particle dynamics at different values of magnetization. At a larger value of coupling parameter, the cluster exhibits a crossover from normal to superdiffusive behaviour with change in magnetic field strength which is a result of the competition between the cyclotron and harmonic

time period. However, at a lower value of coupling parameter the cluster remains subdiffusive at all field strengths. The study brings out several novel features of magnetized dust clusters in complex plasma environments.

4.1 Introduction

Finite clusters can be formed in complex plasma by the charged dust grains and they exhibit different interesting properties which may be relevant to other finite systems like ions in traps, electrons at the surface of liquid He, electrons in quantum dots etc [78, 76, 77]. For example, finite dust clusters exhibit solidlike or liquidlike phases [117, 79], rotation about the symmetry axis [149, 148, 101], concentric circular arrangement of particles [150], "magic" numbered shell configurations [86] and normal modes [88, 82] etc. These clusters consist of a small number of charged dust particles and their behaviour depends strongly on the particle number, strength of particle-particle interaction, confining potential etc. [51].

Collective oscillation processes in finite charged particle clusters have been extensively studied by many groups in the past. Schweigert *et al.* studied the spectral properties of two-dimensional Coulomb clusters [89]. They obtained the ground states and the spectrum of normal modes of two-dimensional clusters formed by charged particles [89]. The normal mode analysis of two- and three-dimensional clusters of charged dust particles has also been reported in various other works [88, 90, 91, 151, 103]. In these works, the analysis was done by solving an eigenvalue equation involving the dynamical matrix thereby finding the mode oscillation patterns and mode frequencies.

The effect of magnetic field on the behaviour of clusters of dust in complex plasma has also been widely investigated previously both via numerical simulation and experiments [101, 100, 104]. It was found in frictionless Molecular Dynamics simulation recently that a three dimensional Yukawa cluster consisting of 32 particles exhibits phase transition from an ordered rotational phase to disordered rotational phase as a function of external magnetic field strength and Coulomb

coupling parameter [152]. Melzer *et al.* studied 2D cluster of 34 dust particles and found to exhibit rotation in the presence of sufficiently strong external magnetic field [103]. Konopka *et al.* observed rigid and sheared rotation of a dusty plasma monolayer in the presence of a perpendicular magnetic field [137]. The shear elastic modulus of the plasma crystal was obtained by using the critical shear stress at which shear-induced melting occurs.

In the present work, normal mode spectra of finite dust cluster in the presence of external magnetic field has been obtained by using Langevin Dynamics simulation for the first time. The results are in good agreement with the dispersion relation obtained from theoretical analysis taking into account Lorentz force. The normal modes in cluster of charged dust particles in the presence of magnetic field has remained an almost unexplored area. Melzer *et al.* experimentally studied the dynamics of 2D cluster of 34 particles in the presence of magnetic field in terms of normal modes that were determined from dynamical matrix [103]. Literature however does not show any simulation or theoretical work related to phonon spectra of finite dust cluster in the presence of magnetic field. Presence of strong magnetic field may affect the trajectories of massive dust particles thus controlling the single particle dynamics as well as pattern of phonon spectra provided cyclotron time scale becomes comparable to harmonic time scale. We also try to find a connection between the self-diffusion of cluster particles and the emergence of new modes with increase in magnetic field strength.

Diffusion in confined geometries is an interesting topic of study. Because the particle motion is restricted in space such systems are expected to show anomalous diffusion behaviour. In some biological systems where particles' motion is restricted anomalous diffusion behaviour is seen. For example, diffusion of tracer particles in crowded environment of living cells is found to be anomalous in length and time scales below a few micrometers and several seconds [153]. Statistical analyses of particle position increments in an experiment on 2D dust cluster suggested the particle dynamics to be superdiffusive on all timescales until the displacements of particles exceed the size of the cluster besides confirming the particle dynamics to have self similar nature [154]. The effect of magnetic field on diffusion of charged particles in plasma has been widely investigated in recent decades via numeri-

cal simulation and laboratory experiments. Ott and Bonitz found that diffusion of dust particles in a 2D strongly coupled magnetized complex plasma exhibits Bohm like $1/B$ dependence in the strong field limit corresponding to both parallel and perpendicular diffusion coefficients [155]. The effect of magnetic field on diffusion of dust particles was investigated in the presence of ion flow and dust-neutral collision via Langevin Dynamics simulations which confirmed the diffusion to be anomalous [156, 157].

The motivation behind the present study is to understand phenomena that may emerge in clusters of charged dust particles under high magnetic field. In a finite dust cluster in complex plasma the application of an external magnetic field introduces a time scale in addition to the already existing time scales i.e, timescales associated with dust neutral collision, confinemnent potential and dust-dust interaction. The competition of the cyclotron timescale with the other timescales may give rise to various intriguing phenomena. It is often difficult to see direct effect of the magnetic field on dust particles due to its large mass. It requires a sufficiently large magnetic field to magnetize the massive dust particles compared to electrons and ions so that the Hall parameter $h = \frac{\Omega_c}{\nu}$ and the magnetization parameter $\beta = \frac{\Omega_c}{\omega_{pd}}$ are of the order 1, Ω_c, ω_{pd} and ν being the dust cyclotron frequency, dust plasma frequency and dust-neutral collision frequency respectively. However, it has now been possible to generate sufficiently high magnetic fields in complex plasma experiments so that dust particles get mangetized [93]. Ordered structures formed by dust particles were observed in the Magnetized Dusty Plasma Experiment (MDPX) which was found to have the same spatial shape as a grid [98] Kählert *et al.* proposed an interesting technique that exploits the frictional coupling between complex plasma and rotating neutral gas that can be used to realize the effect of strong magnetic field on dust particles [94]. The basic idea of this technique is to induce coriolis force that may bring out similar effects as by magnetic Lorentz force. Using this technique they could generate effective magnetic field greater than $10^4\,T$.

The remainder of the chapter is organized as follows. The description of the model is outlined in section 4.2. The details of Langevin Dynamics simulation and the methods adopted to study collective modes are discussed in section 4.3.

The results of linear dust chain and isotropic two-dimensional Yukawa clusters are described in section 4.4 and section 4.5 summarises the findings of this work.

4.2 The Model

We consider a system of N interacting dust particles each having mass m and charge q_d in two dimension immersed in plasma obeying quasineutrality. The interaction among the particles is assumed to be governed by Yukawa potential,

$$V_Y(r) = \frac{q_d}{4\pi\epsilon_0 r}\exp\left(-r/\lambda_d\right), \tag{4.1}$$

where, r is interparticle distance and λ_d is the Debye length for the dust particles. The particles are assumed to be harmonically confined i.e, each dust particle experiences a force due to the harmonic oscillator potential energy,

$$V_C(x,y) = \frac{1}{2}m\Big(\omega_{0x}^2x^2 + \omega_{0y}^2y^2\Big), \tag{4.2}$$

where, ω_{0x} and ω_{0y} are the harmonic confinement strengths along $x-$ and $y-$directions respectively. The confining harmonic potential can be applied in laboratory dusty plasma experiments by using a circular trough or ring in the lower electrode [88, 37]. An external magnetic field acting on the dust particles is also considered in the $z-$ direction.

The equation of motion of the i^{th} particle can thus be written as :

$$\begin{aligned} m\ddot{\mathbf{r}}_i = {} & q_d(\mathbf{v}_i \times \mathbf{B}) - q_d\nabla\sum_{j\neq i}^{N} V(r_{ij}) \\ & - m\omega_{0x}^2x_i\hat{\mathbf{e_x}} - m\omega_{0y}^2y_i\hat{\mathbf{e_y}} - \nu m\dot{\mathbf{r}}_i + \mathbf{A}_i(t), \end{aligned} \tag{4.3}$$

where, $r_{ij} = |\mathbf{r}_i - \mathbf{r}_j|$ is the distance between the ith and jth particles, $\hat{\mathbf{e_x}}$ and $\hat{\mathbf{e_y}}$ are the unit vectors in the $x-$ and $y-$directions respectively, ν is the dust-neutral collision frequency and $\mathbf{A}_i(t)$ denotes the random force acting on the ith dust particle due to collision with the neutrals [119]. The random force term is assumed to obey the following relation according to the fluctuation - dissipation theorem [106],

$$\left\langle A_{ij}(0)A_{ik}(t)\right\rangle = 2m\nu k_BT_d\delta(t)\delta_{jk}, \quad j,k \in \{x,y\} \tag{4.4}$$

where, T_d denotes dust kinetic temperature and $\delta(t)$ is delta function. The present system can be charcterized by four dimensionless parameters, $\Gamma = \frac{q_d^2}{4\pi\epsilon_0 r_0 k_B T_d}$, $\kappa = \frac{r_0}{\lambda_d}$, $\Omega_c' = \frac{q_d B}{m\omega_{0x}}$ and $\nu' = \nu\omega_{0x}^{-1}$. Γ and κ are known as the coupling constant and screening parameters respectively. Ω_c' and ν' denotes the dimensionless magnetic field strength and dimensionless friction coefficient respectively. Here, $r_0 = \left[\frac{2q_d^2}{4\pi\epsilon_0 m\omega_{0x}^2}\right]^{1/3}$ which is the ground state inter-particle distance for a system consisting of two harmonically confined Coulomb interacting particles [109]. The present system can be described in terms of four different time scales : the collision time scale ($\tau_{col} = \frac{1}{\nu}$), the harmonic time scale ($\tau_h = \frac{1}{\omega_{0x}}$), cyclotron time scale ($\tau_c = \frac{2\pi}{\Omega_c}$) and the time scale associated with the interaction among the dust grains defined by the dust plasma frequency ($\tau_{int} = \frac{2\pi}{\omega_{pd}}$). The dust plasma frequency is defined as $\omega_{pd} = \sqrt{\frac{q_d^2}{4\pi\epsilon_0 m a^3}}$ where, a is the average interparticle distance between the dust grains [158].

4.3 Langevin dynamics simulation

Langevin dynamics simulation was performed on a system of 34 Yukawa interacting particles in two dimension confined harmonically in the $x-y$ plane in the presence of an external magnetic field applied along $z-$ direction. The particles are initially randomly distributed inside a square simulation box with random initial velocities. A dimensionless version of Eq. (4.3) has been solved numerically by using the BAOAB algorithm which was shown to perform well in the limits of both low and high friction [121], [106]. In the simulation, time, distance, energy and temperature are scaled respectively by $t_0 = \omega_{0x}^{-1}$, $r_0 = \left[\frac{2q_d^2}{4\pi\epsilon_0 m\omega_{0x}^2}\right]^{1/3}$, $E_0 = \left[\frac{q_d^2 m^{1/2}\omega_{0x}}{4\pi\epsilon_0 2^{1/2}}\right]^{2/3}$ and $T_0 = E_0/k_B$. In our simulation, longitudinal and transverse current autocorrelation functions are evaluated from the knowledge of particle positions and velocities. They are defined as [159],

$$J_L(\mathbf{k},t) = \Big\langle j_L(\mathbf{k},t) j_L(-\mathbf{k},0)\Big\rangle, \tag{4.5}$$

and

$$J_T(\mathbf{k},t) = \Big\langle j_T(\mathbf{k},t) j_T(-\mathbf{k},0)\Big\rangle, \tag{4.6}$$

where, $j_L(\mathbf{k},t)$ and $j_T(\mathbf{k},t)$ are spatial Fourier transform of longitudinal and transverse particle current density and are defined as,

$$j_L(\mathbf{k},t) = \frac{1}{\sqrt{N}} \sum_{i=1}^{N} v_{ix} \exp(i\mathbf{k}\cdot\mathbf{r}_i), \tag{4.7}$$

and

$$j_T(\mathbf{k},t) = \frac{1}{\sqrt{N}} \sum_{i=1}^{N} v_{iy} \exp(i\mathbf{k}\cdot\mathbf{r}_i). \tag{4.8}$$

In the context of our simulation, the angle bracket $\left\langle .. \right\rangle$ denotes average over a sufficiently large number of time origins [106], the wavenumber is chosen to be along $x-$direction i.e, $\mathbf{k} = k\ \hat{\mathbf{e}_\mathbf{x}}$, v_{ix} and v_{iy} denote the $x-$ and $y-$ components of the velocity of the ith particle. The Fourier transform of $J_L(\mathbf{k},t)$ and $J_T(\mathbf{k},t)$ gives the spectrum of longitudinal and transverse modes respectively and defined as,

$$C_L(\mathbf{k},\omega) = \int_{-\infty}^{\infty} J_L(\mathbf{k},t) \exp(i\omega t) dt, \tag{4.9}$$

and,

$$C_T(\mathbf{k},\omega) = \int_{-\infty}^{\infty} J_T(\mathbf{k},t) \exp(i\omega t) dt. \tag{4.10}$$

In our simulation, $C_L(\mathbf{k},\omega)$ and $C_T(\mathbf{k},\omega)$ are obtained by performing discrete Fourier transform on the functions $J_L(\mathbf{k},t)$ and $J_T(\mathbf{k},t)$ for a time interval of $300\,\omega_{0x}^{-1}$. In the process of obtaining the phonon spectrum, a simulation run lasts for 1×10^7 time steps with the value of a time step chosen as $1\times10^{-4}\,\omega_{0x}^{-1}$(except in the run corresponding to $\Omega_c' = 11.33$ and $\Gamma = 7274$ where the time step is chosen as $1.3\times10^{-4}\omega_{0x}^{-1}$). The system of dust particles is first allowed to attain a steady state by collision with the neutrals. This phase lasts for 5×10^6 time steps. The spectrum is obtained from the position and velocity data acquired during the last 5×10^6 steps. While obtaining the time series for Mean Squared Displacement the length of the simulation run is increased up to 1×10^8 time steps and the time step is increased up to $1.3\times10^{-4}\,\omega_{0x}^{-1}$ in order to obtain an extended time series.

4.4 Results and Discussion

The case of a Yukawa cluster consisting of 34 particles was investigated in two different situations. First the longitudinal and transverse current correlation spec-

tra for a linear chain of charged dust particles was obtained in the presence of an external magnetic field and secondly, the spectra of a 2D cluster of particles was obtained and compared them (for both linear chain and 2D cluster) with the dispersion obtained from an analytical model of the cluster under harmonic approximation.

4.4.1 Linear chain in the presence of a perpendicular magnetic field

A linear chain of particles lying along $x-$ direction can be created by making the harmonic confining strength along $y-$ direction (ω_{0y}) sufficiently greater than that along $x-$ direction (ω_{0x}) [160]. In our simulation, the ratio of confining strengths $\alpha_{conf} = \frac{\omega_{0y}}{\omega_{0x}}$ is chosen to be 20. A snapshot of the simulation is shown in Fig. 4.1. The particles can be seen to be lying along a chain, although

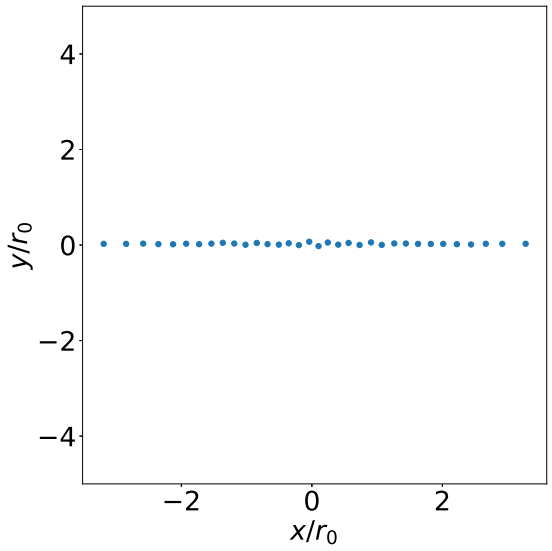

Figure 4.1: A snapshot from the Langevin dynamics simulation of the linear chain of harmonically confined dust particles. The values of the coupling constant, screening parameter and dimensionless friction coefficients respectively are $\Gamma = 2487.67$, $\kappa = 4.32.$ and $\nu' = 0.6$. The value of α_{conf} is chosen to be 20.

some of the particles in the central region shows slight deviation from strict one-dimensional arrangement. Since, the variance of particle positions in $y-$ direction is much smaller than that in $x-$ direction the arrangement of particle positions

can reasonably be considered linear.

Such linear chain of particles have been observed both in experiments and simulations previously in diverse physical systems[161, 162, 163, 164]. Here, we are interested in the behaviour of a chain formed by charged dust particles in complex plasma in the presence of an externally applied perpendicular magnetic field. The longitudinal current correlation spectra of such a chain of particles is shown in Fig. 4.2 at different magnetic field strengths by keeping the coupling and screening parameters fixed. It can be seen that there are two different branches in the spectrum at higher and lower frequencies which are reminiscent of optic and acoustic branches observed in a linear diatomic lattice [165, 166]. The transverse current correlation spectra is shown in Fig. 4.3. To understand the origin of

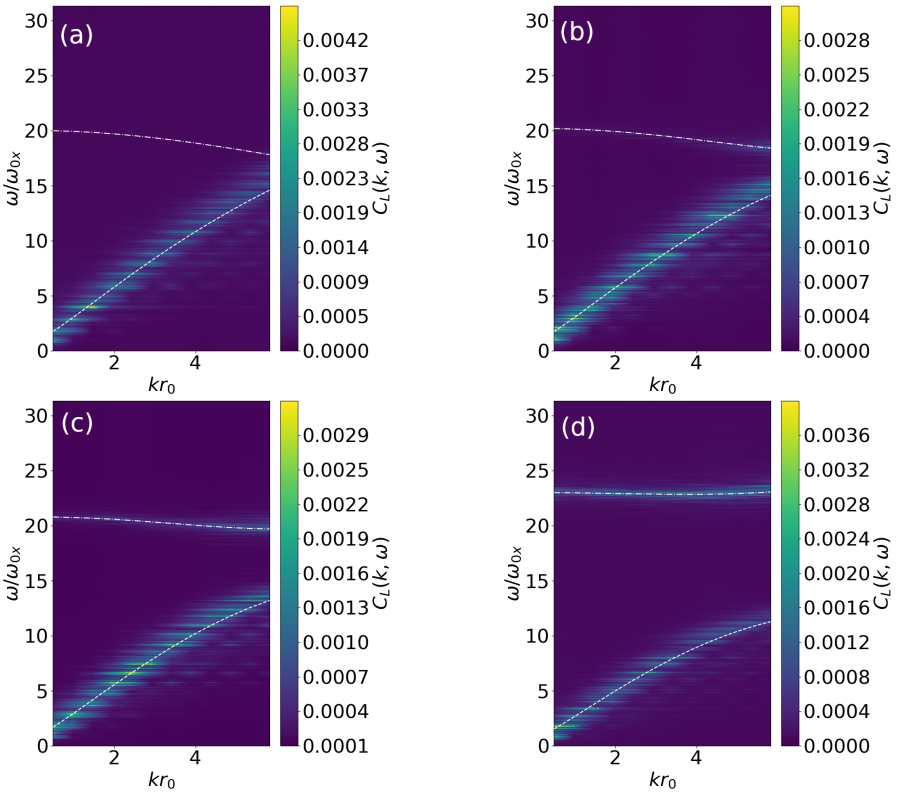

Figure 4.2: Longitudinal current correlation spectra $C_L(\mathbf{k},\omega)$ at different magnetic field strengths a) $\Omega_c' = 0.00$, b) $\Omega_c' = 2.83$, c) $\Omega_c' = 5.67$ and d) $\Omega_c' = 11.33$ with fixed values for other parameters as $\Gamma = 2487.67$, $\kappa = 4.32$ and $\nu' = 0.6$. The white dashed and dash-dot lines respectively denotes the lower and higher frequency branches obtained by numerically solving the dispersion relation (Eq. 4.18).

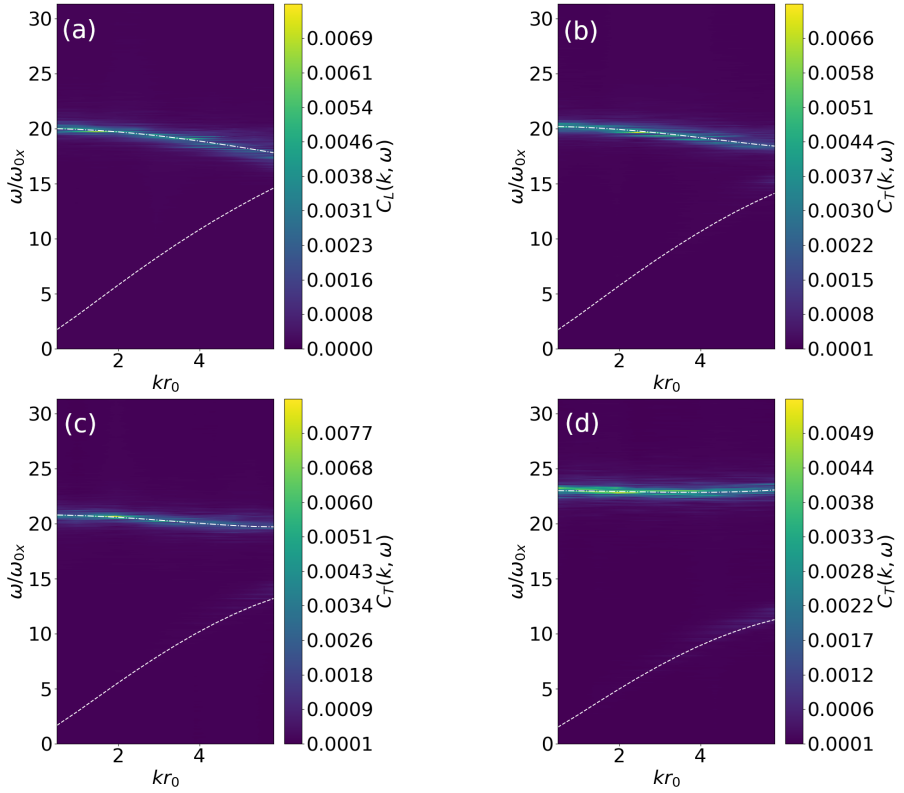

Figure 4.3: Transverse current correlation spectra $C_T(\mathbf{k},\omega)$ at different magnetic field strengths a) $\Omega_c' = 0.00$, b) $\Omega_c' = 2.83$, c) $\Omega_c' = 5.67$ and d) $\Omega_c' = 11.33$ with fixed values for other parameters as $\Gamma = 2487.67$, $\kappa = 4.32$ and $\nu' = 0.6$. The white dashed and dash-dot lines respectively denotes the lower and higher frequency branches obtained by numerically solving the dispersion relation (Eq. 4.18).

the spectra, the dispersion relation is obtained from the equation of motion under the harmonic approximation as outlined below.

Considering the interparticle interaction to be modeled by Yukawa potential (Eq. 4.1), the spring constants along $x-$ and $y-$directions can be obtained by linearizing Yukawa potential as,

$$K_x = \frac{q_d^2}{4\pi\epsilon_0}\Big[\frac{2 + 2j\bar{\kappa} + j^2\bar{\kappa}^2}{j^3 a^3 \exp(j\bar{\kappa})}\Big], \tag{4.11}$$

and

$$K_y = \frac{q_d^2}{4\pi\epsilon_0}\Big[\frac{1 + j\bar{\kappa}}{j^3 a^3 \exp(j\bar{\kappa})}\Big], \tag{4.12}$$

where, $\bar{\kappa} = \frac{a}{\lambda_d}$, a being the distance between two immediate neighbours in equilibrium. In the above, j is a number denoting the index of a particle along the linear chain. The equations of motion along x- and y-directions considering linearized force due to Yukawa interaction,

$$m\ddot{x}_n = \sum_{j=1}^{N_{neigh}} K_x(x_{n+j} + x_{n-j} - 2x_n) + q_d B\dot{y}_n - m\omega_{0x}^2 x_n - m\nu\dot{x}_n, \tag{4.13}$$

$$m\ddot{y}_n = \sum_{j=1}^{N_{neigh}} K_y(y_{n+j} + y_{n-j} - 2y_n) - q_d B\dot{x}_n - m\omega_{0y}^2 y_n - m\nu\dot{y}_n. \tag{4.14}$$

We assume,

$$x_n = x_0 \exp(-i\omega t) \exp(-ikna),$$

and,

$$y_n = y_0 \exp(-i\omega t) \exp(-ikna).$$

By substituting the solutions in the above equations of motion we get,

$$-\omega^2 x_n = -E_1^2 x_n - i\Omega_c \omega y_n + i\omega\nu x_n, \tag{4.15}$$

$$-\omega^2 y_n = -E_2^2 y_n + i\Omega_c \omega x_n + i\omega\nu y_n. \tag{4.16}$$

Here,

$$E_1^2 \;=\; \omega_{0x}^2 + \sum_{j=1}^{N_{neigh}} \frac{4K_x}{m} \sin^2(kja/2),$$

and,

$$E_2^2 = \omega_{0y}^2 - \sum_{j=1}^{N_{neigh}} \frac{4K_y}{m} \sin^2(kja/2),$$

where, N_{neigh} denotes the number of neighbors considered for interaction with the nth particle.

These two equations can be written in matrix form,

$$A \begin{bmatrix} x_n \\ y_n \end{bmatrix} = 0, \tag{4.17}$$

where,

$$A = \begin{bmatrix} (-\omega^2 + E_1^2 - i\omega\nu) & i\omega\Omega_c \\ -i\omega\Omega_c & (-\omega^2 + E_2^2 - i\omega\nu) \end{bmatrix}.$$

The dispersion relation is obtained by letting the determinant of A vanish, i.e,

$$(-\omega^2 + E_1^2 - i\omega\nu)(-\omega^2 + E_2^2 - i\omega\nu) - (\omega\Omega_c)^2 = 0. \tag{4.18}$$

The phonon spectra obtained from longitudinal and transverse current autocorrelation functions are shown in Fig. 4.2 and Fig. 4.3 respectively. The results are compared with the frequency branches obtained from the numerical solution of the dispersion relation Eq. 4.18. For $\mathbf{B} \to 0$ the results agree with that reported by Liu *et al.* for 1D chain formed in complex plasma [81]. In the absence of an external magnetic field the longitudinal phonon spectrum consists only of the acoustic branch (as seen from Fig. 4.2). But as the magnetic field strength is increased, the longitudinal phonon spectrum starts showing both acoustic and optic branch. This can be attributed to the increased localization of the particles' motion with the increase of the magnetic field strength. On the contrary, the transverse phonon spectrum consists only of the optic branch at all the field strengths (Fig. 4.3). Piacente *et al.* observed that on increasing magnetic field strength to sufficiently large values the frequency of the optical branch approaches cyclotron frequency [167]. In our case, although the frequency of the optical branch increases with increase in the magnetic field strength for all values of dimensionless wavenumber kr_0, the frequency remains always higher than the cyclotron frequency. It can be seen that, at zero wavenumber the acoustic mode freqency is zero and the optical

mode frequency is $20\,\omega_{0x}$ which is the same as harmonic confining strength along $y-$direction. This zero wavenumber mode indicates a sloshing oscillation of the cluster at $\omega = \omega_{0y} = 20\,\omega_{0x}$. As the wavenumber is increased, the repulsive Yukawa interaction starts playing a dominant role and the frequency of the optical mode decreases. A similar observation was reported by Liu *et al.* [81].

4.4.2 2D Yukawa cluster in the presence of a perpendicular magnetic field

In dusty plasma experiments, dust particles can be trapped to form two-dimensional layer in the sheath region of radiofrequency (rf) discharge due to the balance between gravity and electric field force [82]. In MD simulation such a system can be acheived by applying harmonic confinement in the form of a potential described by Eq. 4.2. An external magnetic field is applied along $z-$direction perpendicular to the cluster. The ratio of confining strength $\alpha_{conf} = \frac{\omega_{0y}}{\omega_{0x}}$ is chosen to be 1 so that an isotropic cluster is formed as shown in Fig. 4.4. For the results of isotropic 2D cluster in this study the dimensionless friction coefficient is fixed as $\nu' = 0.12$ except for Fig. 4.12(c) and 4.12(d) where it is fixed as $\nu' = 3.84$. The value of confinement strengths are chosen as $\omega_{0x} = \omega_{0y} = 25\ s^{-1}$.

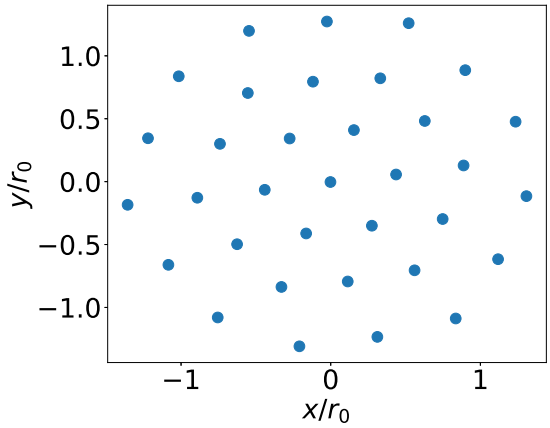

Figure 4.4: Snapshot of a two-dimensional Yukawa cluster consisting of $N = 34$ particles obtained from Langevin dynamics simulation at zero external magnetic field with $\Gamma = 7274$ and $\kappa = 4.7$.

The trajectory of an arbitrarily chosen particle from a harmonically confined clus-

ter of 34 Yukawa interacting particles is shown in Fig. 4.5 at different strengths of transverse external magnetic field. It is clear from the trajectories that on increasing the magnetic field strength the particles start exhibiting Larmor oscillation about the magnetic field in perpendicular direction. This is evident from the fact that the trajectories curls up with the increase of the magnetic field strength. Dusty plasma like other many body systems support variety of col-

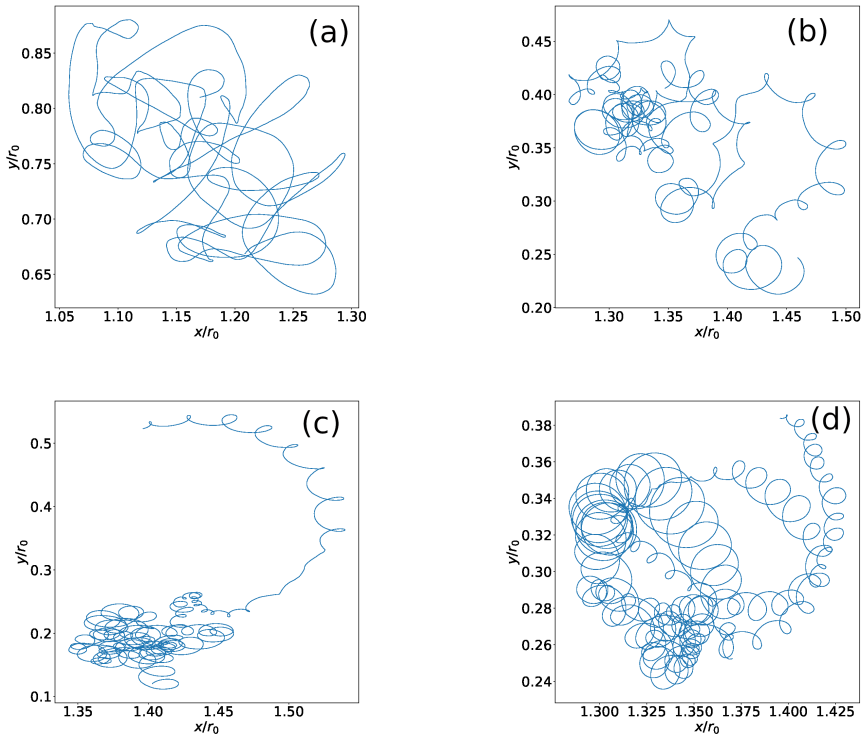

Figure 4.5: Trajectory of an arbitrarily chosen particle at different magnetic field strengths, a) $\Omega_c' = 1.13$, b) $\Omega_c' = 5.67$, c) $\Omega_c' = 7.93$ and d) $\Omega_c' = 11.33$ keeping coupling and screening parameter fixed at $\Gamma = 145.48$ and $\kappa = 4.7$ respectively. The trajectories are plotted for a time duration of $7.5\,\omega_{0x}^{-1}$.

lective modes. Dust acoustic waves, dust density waves, dust cyclotron waves are some of the low frequency waves exhibited by dusty plasma in weakly coupled state whereas dust lattice wave arises in strongly coupled solid like state. The 2D dusty plasmas in strongly coupled solid like regime are known to exhibit compressional or longitudinal waves with direction of oscillation along the wave propagation direction. While longitudinal waves arise in gaseous state, transverse

waves are characteristic feature of strongly correlated system. The purpose of the present work is to find the phonon spectra of magnetized dust cluster which will help in understanding the dynamical behaviour of such a system with increasing magnetic field.

Phonon spectrum

The longitudinal and transverse current correlation spectra of a cluster of 34 particles are shown in Fig. 4.6 at two different coupling strengths ($\Gamma = 7274$ and $\Gamma = 145.48$) at zero external magnetic field. The spectra at $\Gamma = 7274$ suggests the presence of solid like order in the cluster whereas, at $\Gamma = 145.48$ the system is in a partially melted state as was observed in bulk 2D complex plasma by Nunomura *et al.* [168]. The longitudinal current correlation spectra of a 2D

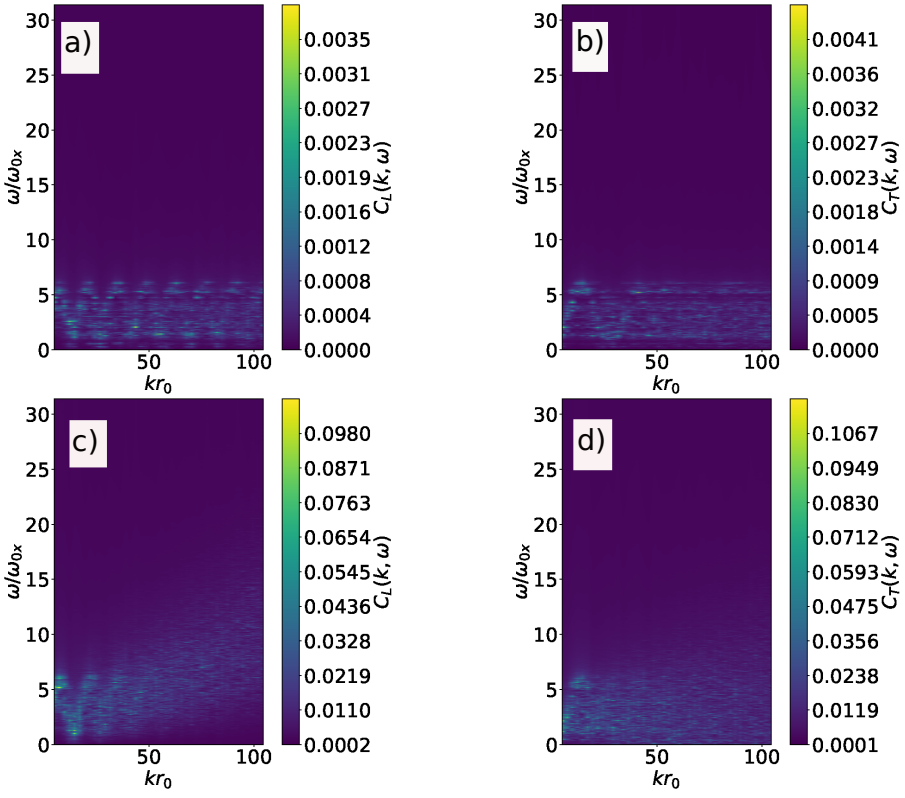

Figure 4.6: Current correlation spectra for longitudinal and transverse modes reflecting the phase state of the cluster ($N = 34$) at two different value of coupling strengths, $\Gamma = 7274$ [a) and b)] and $\Gamma = 145.48$ [c) and d)] at zero external magnetic field and $\kappa = 4.7$.

Yukawa cluster is shown in Fig. 4.7 for $\Gamma = 7274$ at different values of magnetic field strengths denoted by Ω_c'. The longitudinal mode is excited at $\sim 6\omega_{0x} = 150\ rad/s$ corresponding to $kr_0 \sim 15$ at $\Omega_c' = 0$. The increase in the disturbance of the mode at $\Omega_c' = 0.11$ may be due to the onset of a new mode in the presence of a magnetic field. This becomes clear in Fig. 4.7(c) corresponding to $\Omega_c' = 5.67$ where the original normal mode arising due to thermal effects split into two distinct modes. In order to understand the origin of the spectra the dispersion relation for the system is obtained by assuming a linearized Yukawa interaction potential among the particles.

We assume a monolayer of dust particles having a hexagonal lattice structure with lattice parameter a. So, considering a particle to be lying at $(0, 0)$, the positions of its nearest neighbours are, $(a, 0)$, $(-a, 0)$, $(a/2, \sqrt{3}a/2)$, $(-a/2, \sqrt{3}a/2)$, $(a/2, -\sqrt{3}a/2)$ and $(-a/2, -\sqrt{3}a/2)$. Using harmonic approximation, the Yukawa potential (Eq. 4.1) can be written as,

$$V_Y(r) = \frac{1}{2}K(r-a)^2, \tag{4.19}$$

where, K is the spring constant and defined as,

$$K = \frac{q_d^2}{4\pi\epsilon_0\lambda_d^3}\frac{(2+2\bar{\kappa}+\bar{\kappa}^2)}{\bar{\kappa}^3}\exp(-\bar{\kappa}). \tag{4.20}$$

In the above, $\bar{\kappa} = \frac{a}{\lambda_d}$. Taking into account the force due to all the nearest neighbour particles, the magnetic Lorentz force due to a perpendicular magnetic field, confining harmonic force and the frictional drag force due to the neutrals, the $x-$ and $y-$ components of force on the (s, l) particle of the monolayer can be represented respectively as [169],

$$\begin{aligned} m\ddot{\zeta}_{s,l} = {} & K\sum_{i=1}^{2}(-1)^{i+1}(r_i - a)\frac{a+\Delta\zeta_i}{r_i} \\ & + K\sum_{i=3}^{6}(-1)^{i+1}(r_i - a)\frac{a/2+\Delta\zeta_i}{r_i} \\ & + q_d B\dot{\eta}_{s,l} - m\omega_{0x}^2\zeta_{s,l} - m\nu\dot{\zeta}_{s,l}, \end{aligned}$$

and,

$$
\begin{aligned}
m\ddot{\eta}_{s,l} = K\sum_{i=1}^{2}(-1)^{i+1}(r_i - a)\frac{\Delta\eta_i}{r_i} \\
+ K\Big[(r_3 - a)\frac{\sqrt{3}a/2 + \Delta\eta_3}{r_3} - (r_4 - a)\frac{\sqrt{3}a/2 - \Delta\eta_4}{r_4}\Big] \\
+ K\Big[(r_5 - a)\frac{\sqrt{3}a/2 - \Delta\eta_5}{r_5} - (r_6 - a)\frac{\sqrt{3}a/2 + \Delta\eta_6}{r_6}\Big] \\
- q_d B\dot{\zeta}_{s,l} - m\omega_{0y}^2\eta_{s,l} - m\nu\dot{\eta}_{s,l}.
\end{aligned}
$$

In the above two equations, the displacements of the particles from equilibrium positions along $x-$ and $y-$ directions are denoted respectively by $\zeta_{s,l}$ and $\eta_{s,l}$ and the particle indices along $x-$ and $y-$ directions are denoted by s and l respectively. Also, $\Delta\zeta_i$ and $\Delta\eta_i$ are [170],

$$
\begin{aligned}
\Delta\zeta_1 = \zeta_{s+1,l} - \zeta_{s,l},\ \Delta\eta_1 = \eta_{s+1,l} - \eta_{s,l}, \\
\Delta\zeta_2 = \zeta_{s,l} - \zeta_{s-1,l},\ \Delta\eta_2 = \eta_{s,l} - \eta_{s-1,l}, \\
\Delta\zeta_3 = \zeta_{s+1/2,l+\sqrt{3}/2} - \zeta_{s,l},\ \Delta\eta_3 = \eta_{s+1/2,l+\sqrt{3}/2} - \eta_{s,l}, \\
\Delta\zeta_4 = \zeta_{s,l} - \zeta_{s-1/2,l+\sqrt{3}/2},\ \Delta\eta_4 = \eta_{s-1/2,l+\sqrt{3}/2} - \eta_{s,l}, \\
\Delta\zeta_5 = \zeta_{s+1/2,l-\sqrt{3}/2} - \zeta_{s,l},\ \Delta\eta_5 = \eta_{s,l} - \eta_{s+1/2,l-\sqrt{3}/2}, \\
\Delta\zeta_6 = \zeta_{s,l} - \zeta_{s-1/2,l-\sqrt{3}/2},\ \Delta\eta_6 = \eta_{s,l} - \eta_{s-1/2,l-\sqrt{3}/2}.
\end{aligned}
$$

Considering the displacements to be much smaller than the equlibrium interparticle distance a, i.e, $\Delta\zeta_i << a$ and $\Delta\eta_i << a$ the force equation along $x-$direction becomes,

$$
\begin{aligned}
m\frac{d^2\zeta_{s,l}}{dt^2} = K\Big[\Delta\zeta_1 - \Delta\zeta_2 + \frac{1}{4}(\Delta\zeta_3 - \Delta\zeta_4 \\
+ \Delta\zeta_5 - \Delta\zeta_6) + \frac{\sqrt{3}}{4}(\Delta\eta_3 - \Delta\eta_4 \\
+ \Delta\eta_5 - \Delta\eta_6)\Big] - m\omega_{0x}^2\zeta_{s,l} \\
+ q_d B\frac{d\eta_{s,l}}{dt} - m\nu\frac{d\zeta_{s,l}}{dt},
\end{aligned}
\tag{4.21}
$$

and along $y-$direction,

$$\begin{aligned} m\frac{d^2\eta_{s,l}}{dt^2} &= K\Big[\frac{3}{4}(\Delta\eta_3+\Delta\eta_4-\Delta\eta_5-\Delta\eta_6) \\ &+ \frac{\sqrt{3}}{4}(\Delta\zeta_3+\Delta\zeta_4-\Delta\zeta_5-\Delta\zeta_6)\Big] \\ &- m\omega_{0y}^2\eta_{s,l} - q_dB\frac{d\zeta_{s,l}}{dt} - m\nu\frac{d\eta_{s,l}}{dt}. \end{aligned} \tag{4.22}$$

Now, considering longitudinal oscillation we assume the following two solutions

$$\zeta_{s,l} = \zeta_0 \exp(-i\omega t)\exp(ikas), \tag{4.23}$$

and,

$$\eta_{s,l} = \eta_0 \exp(-i\omega t)\exp(ikas). \tag{4.24}$$

Using these two solutions in Eq. (4.21) and (4.22) the following two equations are obtained,

$$\Big(\omega^2-\omega_{0x}^2+i\omega\nu+C_1\Big)\zeta_{s,l} - i\omega\Omega_c\eta_{s,l} = 0, \tag{4.25}$$

and,

$$i\omega\Omega_c\zeta_{s,l} + \Big(\omega^2-\omega_{0y}^2+i\omega\nu+C_2\Big)\eta_{s,l} = 0, \tag{4.26}$$

In the above the constants C_1 and C_2 are as follows,

$$C_1 \;=\; -2\frac{K}{m}\Big(2\sin^2(ka/2)+\sin^2(ka/4)\Big),$$

and,

$$C_2 \;=\; -6\frac{K}{m}\sin^2(ka/4).$$

By arranging the Eq. 4.25 and 4.26 in matrix form,

$$D\begin{bmatrix}\zeta_{s,l}\\ \eta_{s,l}\end{bmatrix} = 0, \tag{4.27}$$

where,

$$D = \begin{bmatrix}\Big(\omega^2-\omega_{0x}^2+i\omega\nu+C_1\Big) & -i\omega\Omega_c \\ i\omega\Omega_c & \Big(\omega^2-\omega_{0y}^2+i\omega\nu+C_2\Big)\end{bmatrix}.$$

The dispersion relation is obtained by using the condition that the determinant of the coefficient matrix D in Eq. 4.27 should vanish for solutions to exist. This leads to the dispersion relation as follows,

$$\Big(\omega^2-\omega_{0x}^2+i\omega\nu+C_1\Big)\Big(\omega^2-\omega_{0y}^2+i\omega\nu+C_2\Big) - (\omega\Omega_c)^2 = 0. \tag{4.28}$$

This dispersion relation is similar to that obtained by Farokhi *et al.* for bulk 2D dusty plasma in the presence of an externally applied perpendicular magnetic field with a modification due to the harmonic confining term [170].

Assuming the frequency ω to be consisting of real and imaginary parts, i.e, taking $\omega = \omega_r + i\omega_i$ and substituting in Eq. 4.28 a system of two non-linear equations is obtained as follows,

$$(\omega_r^2 - \omega_i\nu + C_1 - \omega_{0x}^2)(\omega_r^2 - \omega_i\nu + C_2 - \omega_{0y}^2) \\ -4(\omega_i + \frac{\nu}{2})^2\omega_r^2 - (\omega_r^2\Omega_c^2) = 0, \tag{4.29}$$

$$(\omega_i + \frac{\nu}{2})\omega_r(2\omega_r^2 - 2\omega_i\nu + C_1 + C_2 - \omega_{0x}^2 - \omega_{0y}^2) - \omega_r\omega_i\Omega_c^2 = 0. \tag{4.30}$$

In the above, the imaginary part of the frequency ω_i is assumed to be much smaller than the real part ω_r so that $\omega_i^2 \sim 0$. These two equations are solved numerically to obtain the frequencies at different values of wavenumber. Frequency vs wavenumber plots are shown in Fig. 4.7 and 4.8 along with longitudinal and transverse current correlation spectra obtained from simulation at $\Gamma = 7274$ and $\kappa = 4.7$ respectively. It is seen from the plots that the dispersion obtained from the analytical model shows good agreement with $C_L(\mathbf{k}, \omega)$ and $C_T(\mathbf{k}, \omega)$ obtained from simulation. In Fig. 4.7 the longitudinal phonon spectrum has been shown at four different magnetic field strengths keeping the coupling parameter and screening parameter fixed. The modes predicted by Eq. 4.29 and 4.30 are superposition of longitudinal and transverse vibrations. One of these have more longitudinal character thus agreeing with the longitudinal current correlation spectra of Fig. 4.7(a). On increasing the magnetic field up to $\Omega_c' = 11.33$ the frequency of the upper branch of the spectra becomes of the order of the cyclotron frequency. The vibrational mode with lower frequency gets quenched at the cost of cyclotron mode.

The transverse phonon spectrum is shown in Fig. 4.8 at four different magnetic field strengths. It is seen that the spectra resembles quite well with the theoretical dispersion curves. The pure longitudinal and transverse modes of magnetized dust cluster can be thought of as the superposition of thermally excited vibrational modes and magnetic field induced cyclotron mode.

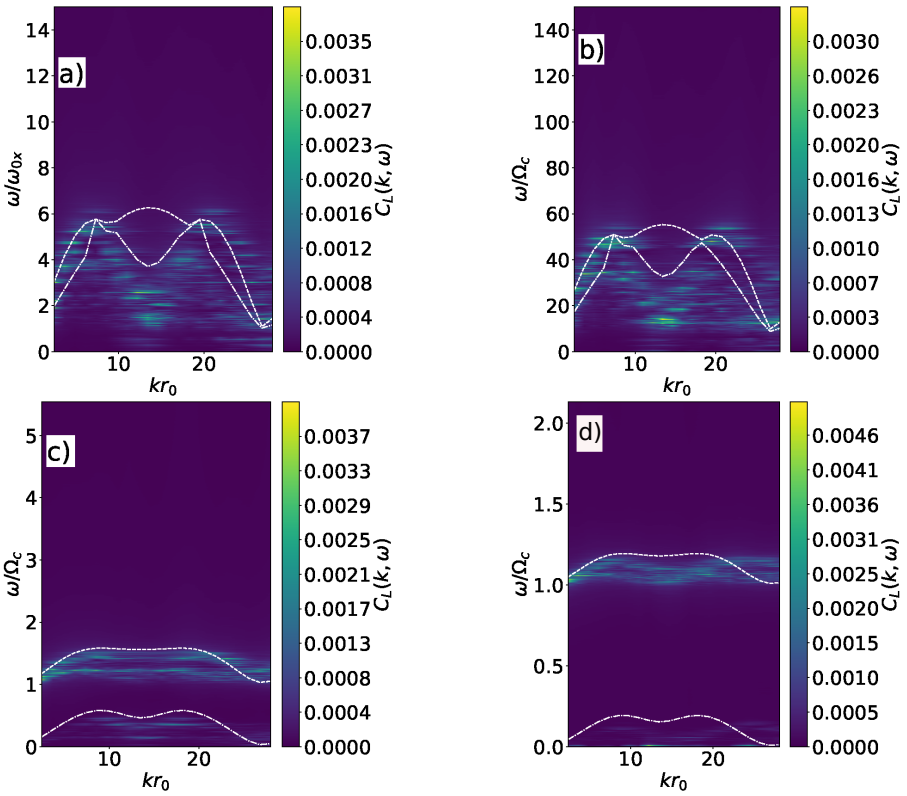

Figure 4.7: Current correlation spectra for longitudinal modes for different values of magnetic field strengths, a) $\Omega_c' = 0$, b) $\Omega_c' = 0.11$, c) $\Omega_c' = 5.67$ and d) $\Omega_c' = 11.33$ at $\Gamma = 7274$ and $\kappa = 4.7$. The white dashed curve denotes the higher frequency branch and the dash-dotted curve denotes the lower frequency branch obtained from analytical calculation.

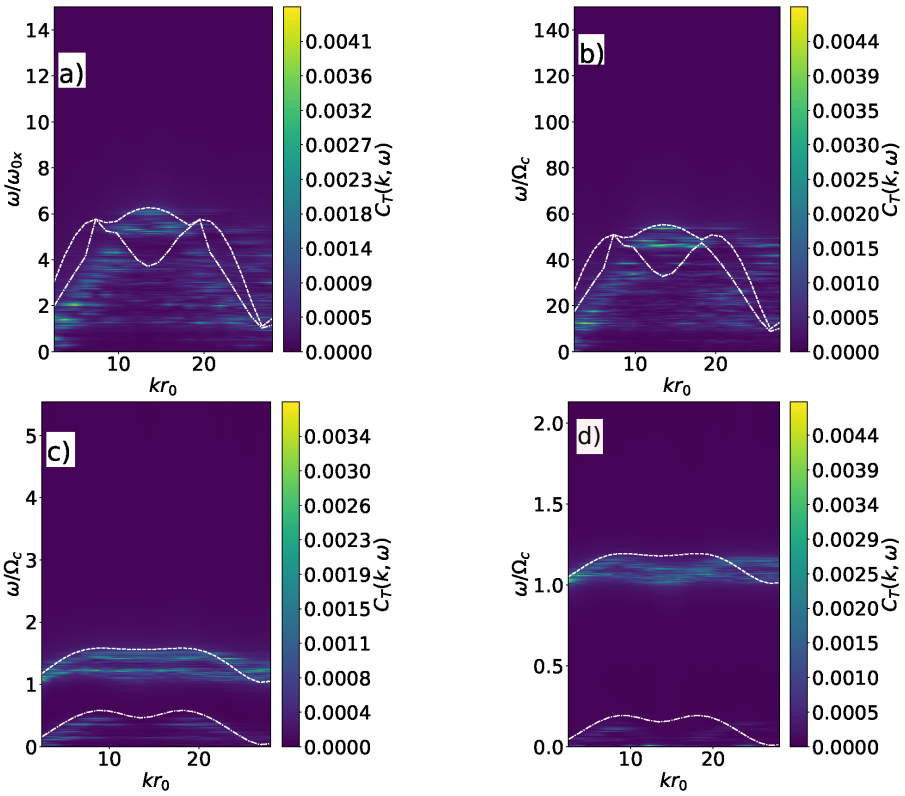

Figure 4.8: Transverse current autocorrelation spectra for different values of magnetic field strengths, a) $\Omega_c' = 0$, b) $\Omega_c' = 0.11$, c) $\Omega_c' = 5.67$ and d) $\Omega_c' = 11.33$ at $\Gamma = 7274$ and $\kappa = 4.7$. The white dashed curve denotes the higher frequency branch and the dash-dotted curve denotes the lower frequency branch obtained from analytical calculation.

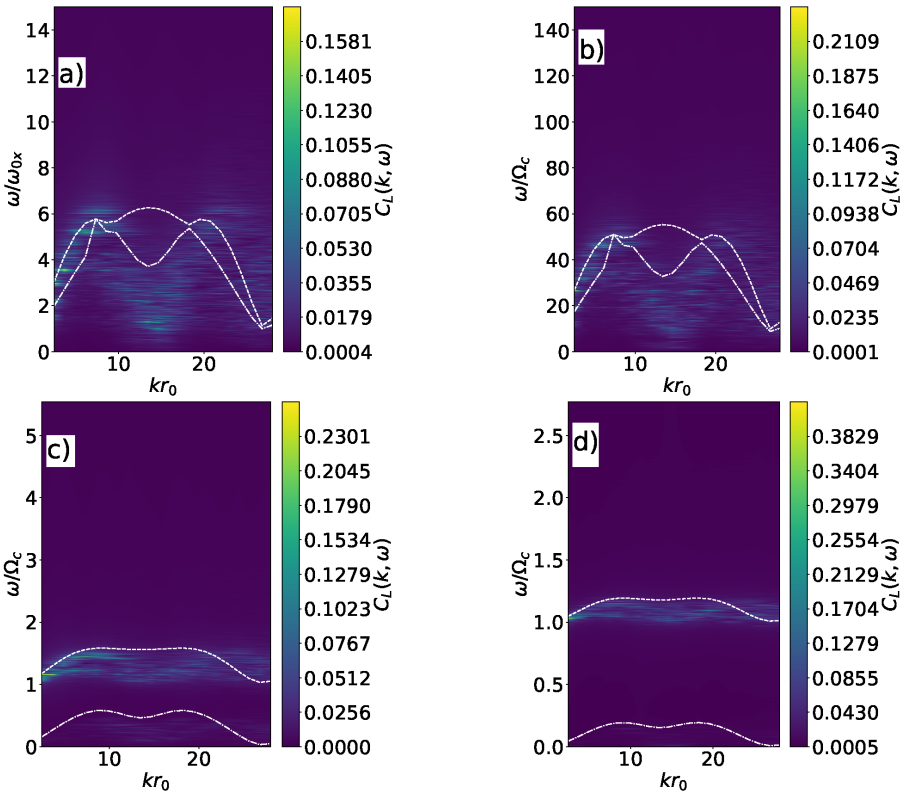

Figure 4.9: Current autocorrelation spectra for longitudinal modes for different values of magnetic field strengths, a) $\Omega_c' = 0$, b) $\Omega_c' = 0.11$, c) $\Omega_c' = 5.67$ and d) $\Omega_c' = 11.33$ at $\Gamma = 145.48$ and $\kappa = 4.7$ respectively. The white dashed curve denotes the higher frequency branch and the dash-dotted curve denotes the lower frequency branch.

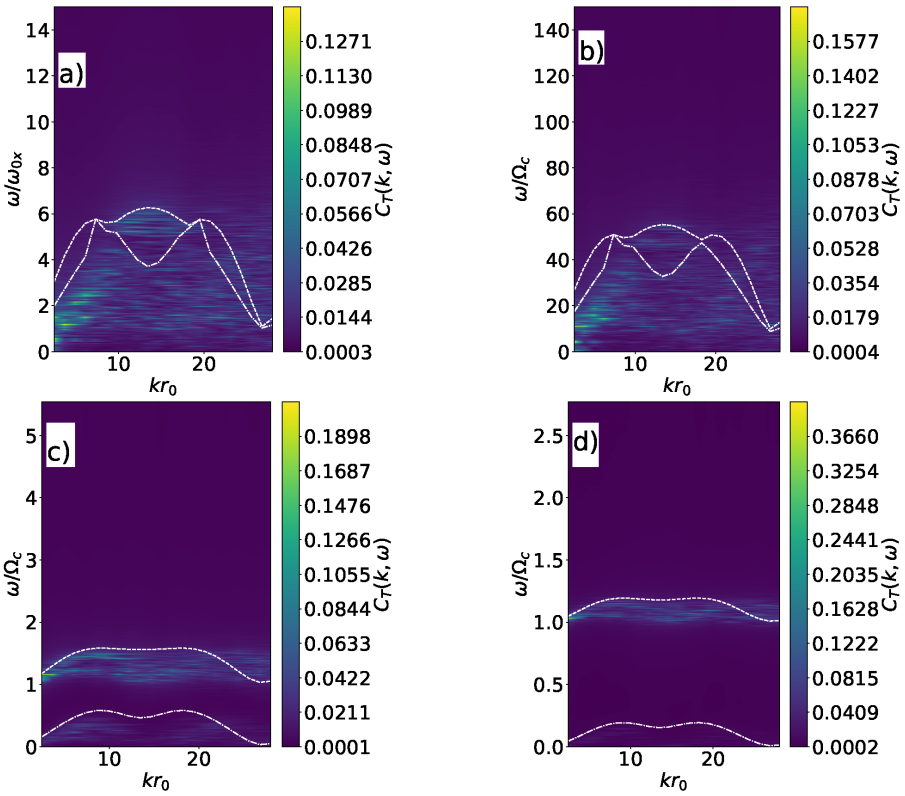

Figure 4.10: Transverse current autocorrelation spectra for different values of magnetic field strengths, a) $\Omega_c' = 0$, b) $\Omega_c' = 0.11$, c) $\Omega_c' = 5.67$ and d) $\Omega_c' = 11.33$ at $\Gamma = 145.48$ and $\kappa = 4.7$ respectively. The white dashed curve denotes the higher frequency branch and the dash-dotted curve denotes the lower frequency branch.

To understand the effect of variation of coupling strength the longitudinal and transverse phonon spectra have been obtained and shown in Fig. 4.9 and 4.10 respectively for $\Gamma = 145.48$ by keeping screening parameter fixed as $\kappa = 4.7$. It is evident from the limits on color scales in these figures that the maximum values of $C_L(\mathbf{k}, \omega)$ and $C_T(\mathbf{k}, \omega)$ increases with decreasing coupling strength which is due to the increase in thermal velocity of the particles with decreasing coupling strength or increase in dust kinetic temperature.

Zhdanov *et al.* experimentally studied the wave spectra of a dusty plasma monolayer considering the particles to be Yukawa interacting [171]. They observed two branches in the spectrum with mixed transverse and longitudinal polarization for waves propagating in different directions with respect to the crystal axis. We observe two branches in the spectrum too, both in theory and simulation. It is seen that, with increase in the magnetic field strength the frequency of the higher frequency branch approaches cyclotron frequency. This happens in both the longitudinal and transverse spectra as the magnetic field is applied in the z-direction which does not introduce any preferred direction into the 2D system. Uchida *et al.* investigated the wave spectra of a strongly coupled bulk 2D plasma crystal in the presence of an external magnetic field [158]. They found the spectra to consist of high and low frequency branches each having both longitudinal and transverse character.

The observed magnetic field effects can be viewed as a result of competition between cyclotron and interaction timescales. When the external magnetic field strength is zero, the spectrum is mainly dominated by the interaction timescale (τ_{int}) defined by the dust plasma frequency (panel (a) in Fig. 4.7 - 4.10). At a non-zero but smaller magnetic field strength (panel (b) in Fig. 4.7 - 4.10) the spectrum is still dominated by the interaction timescale. Only at a sufficiently large value of the field strength the spectrum is governed by the cyclotron timescale. To better understand this fact, the longitudinal phonon spectra obtained from the simulation along with the dispersion curves obtained from analytical calculation are shown in Fig. 4.11 at four different magnetic field strengths. It is seen that when the magnetic field strength is smaller such that $\Omega_c < \omega_{pd}$ [Fig. 4.11(a) and (b)] the modes are distributed over a continuous range of frequencies.

A distinct change in the spectra can be seen when $\Omega_c \sim \omega_{pd}$ [Fig. 4.11(c)] and the spectra becomes separated into two distinct branches when $\Omega_c > \omega_{pd}$ [Fig. 4.11(d)]. This, therefore, indicates the presence of two different timescale regimes in the cluster at low neutral friction: the interaction dominated regime characterized by $\omega_{pd} > \Omega_c$ and the magnetic field dominated regime characterized by $\Omega_c > \omega_{pd}$. However, the distinct phonon spectra are found to disappear when

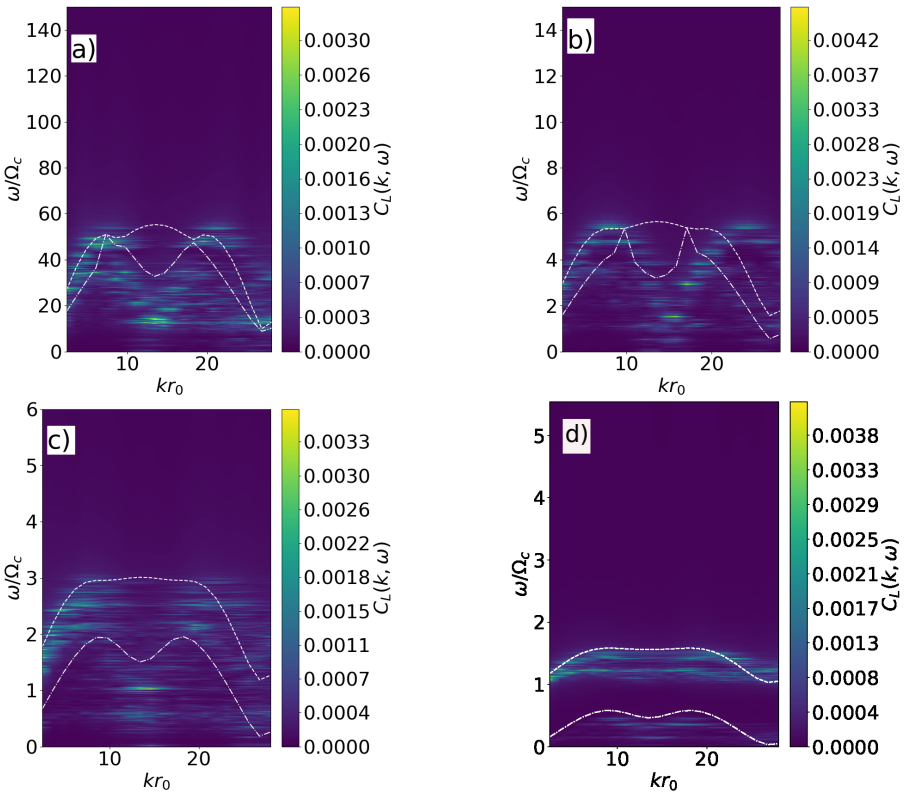

Figure 4.11: Longitudinal current correlation spectra at different values of magnetic field strengths, a) $\frac{\Omega_c}{\omega_{pd}} = 0.05$, b) $\frac{\Omega_c}{\omega_{pd}} = 0.50$, c) $\frac{\Omega_c}{\omega_{pd}} = 1.01$, d) $\frac{\Omega_c}{\omega_{pd}} = 2.52$. The coupling and screening parameters are fixed as $\Gamma = 7274$ and $\kappa = 4.7$ respectively.

the friction coefficient ν becomes greater than the dust plasma frequency ω_{pd} as shown in Fig. 4.12.

To understand the effect of variation of particle number in the cluster, the longitudinal and transverse phonon spectra have been plotted for three different particle numbers $N = 50, 100$ and 300 as shown in Fig. 4.13. It is seen that with increase in the number of particles the peak frequency increases. The snapshots of particle

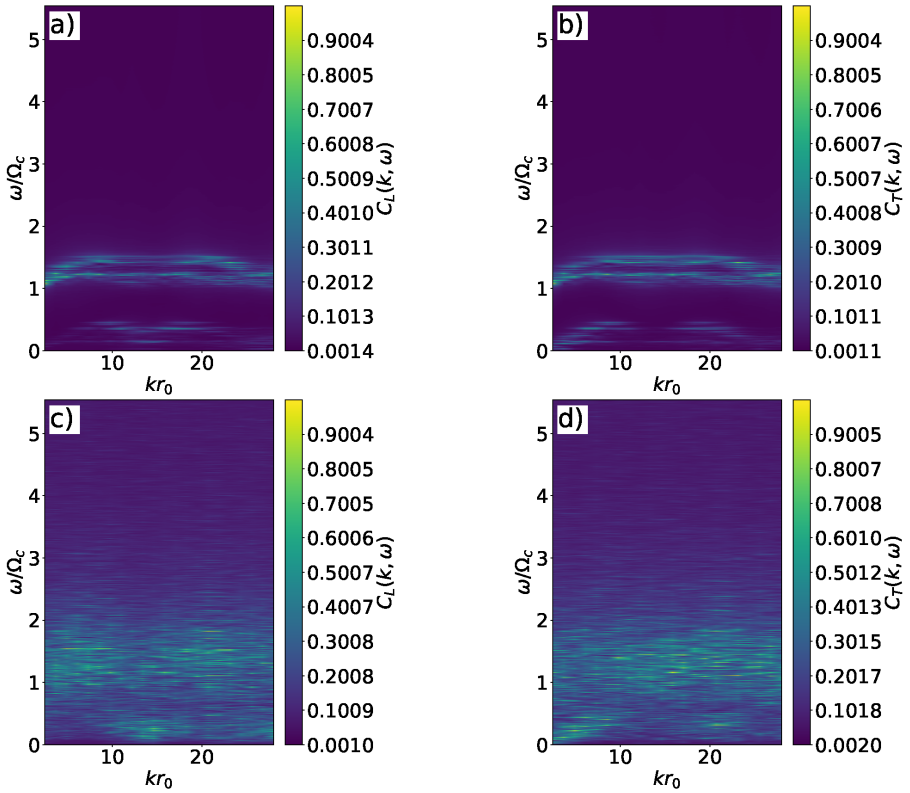

Figure 4.12: Longitudinal and transverse current correlation spectra at dimensionless friction coefficients $\nu' = 0.12$ [a) and b)] and $\nu' = 3.84$ [c) and d)] at fixed value of magnetic field strength $\Omega_c' = 5.67$. The corresponding values of friction coefficients when scaled by dust plasma frequency becomes $\frac{\nu}{\omega_{pd}} = 0.05$ [a) and b)] and $\frac{\nu}{\omega_{pd}} = 1.71$ [c) and d)]. The color scales have been scaled by the maximum values of $C_L(\mathbf{k},\omega)$ and $C_T(\mathbf{k},\omega)$ so that they become uniform. The coupling and screening strengths are fixed at $\Gamma = 7274$ and $\kappa = 4.7$ respectively.

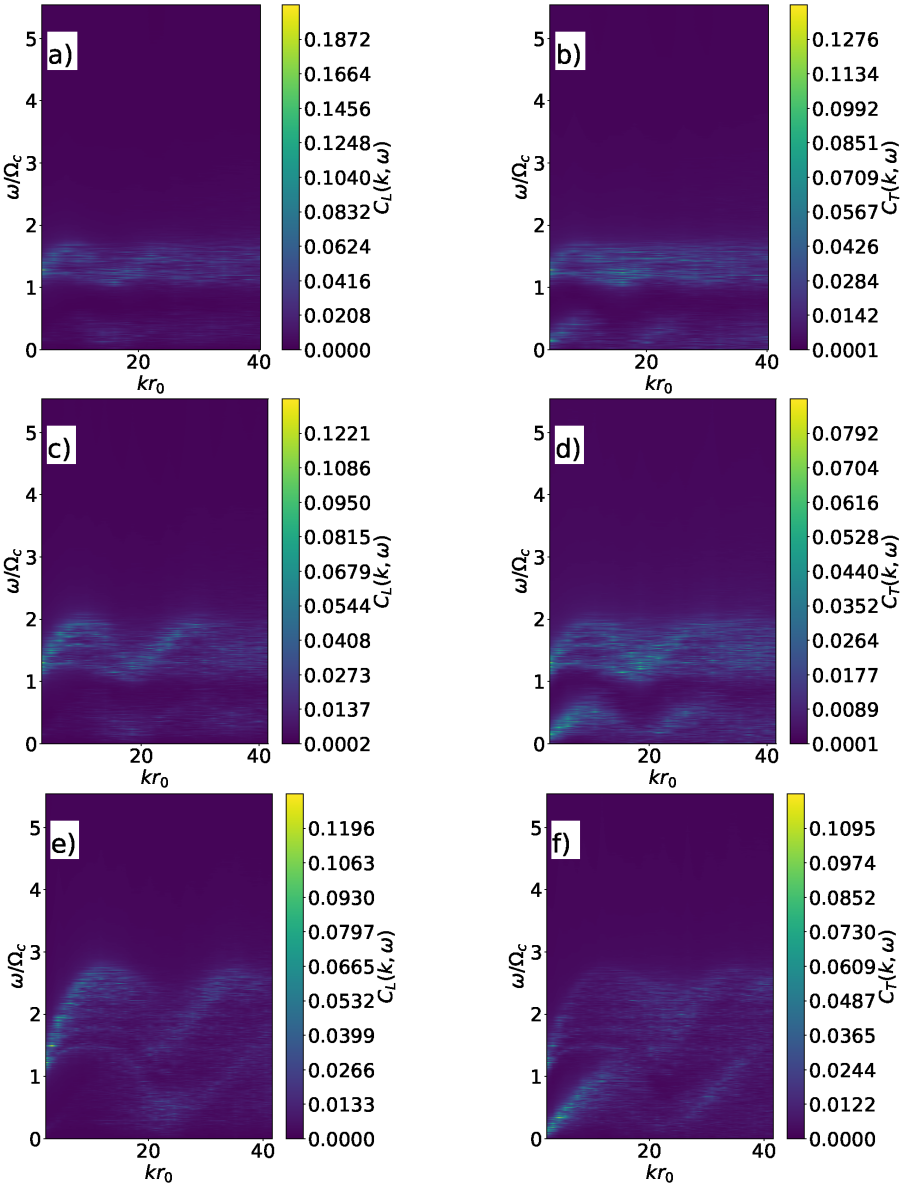

Figure 4.13: Longitudinal and transverse current correlation spectra for different total number of particles, $N = 50$ [a) and b)], $N = 100$ [c) and d)], $N = 300$ [e) and f)] . The dimensionless magnetic field strength, coupling parameter and screening parameters are fixed as $\Omega_c' = 5.67$, $\Gamma = 145.48$ and $\kappa = 4.7$ respectively.

positions have been shown in Fig. 4.14 for different total number of particles in the cluster. Clusters with small number of particles are characterized by nested circular shells whereas with increase in the number of particles hexagonal structure starts appearing in the inner region of the cluster. However, near the outer boundary of the cluster the particles still arrange themselves into circular shells [172].

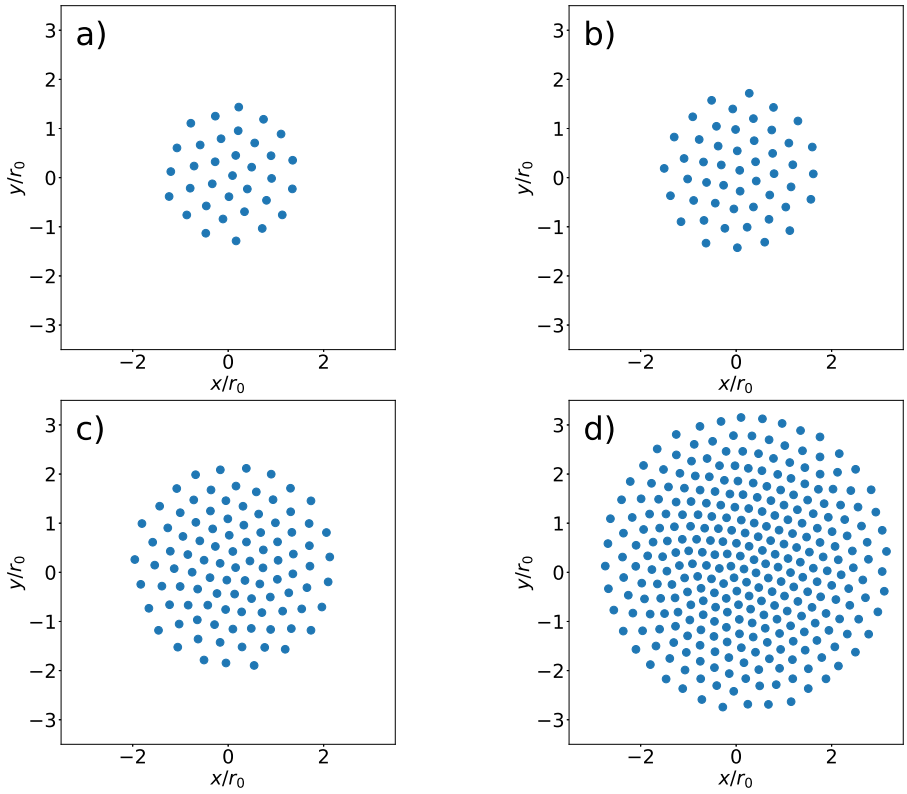

Figure 4.14: Snapshot of particle positions taken at the final timestep of the simualation at different values of total number of particles, a) $N = 34$, b) $N = 50$, c) $N = 100$ and d) $N = 300$ with $\Gamma = 145.48$, $\kappa = 4.7$ and $\Omega_c' = 5.67$.

The Fourier transform of the velocity autocorrelation function is shown in Fig. 4.15 at four different magnetic field strengths. This gives the vibrational Density of States (DoS) [119]. In our simulation, the velocity aucorrelation function is defined as $\frac{1}{N}\langle \sum_{i=1}^{N} \mathbf{v}_i(t) \cdot \mathbf{v}_i(0) \rangle$, where $\langle .. \rangle$ denotes average over time origins. At a lower value of magnetic field strength (say, $\Omega_c' = 0.11$) the phonon states are distributed over a continuous range of frequencies. But as the magnetic field

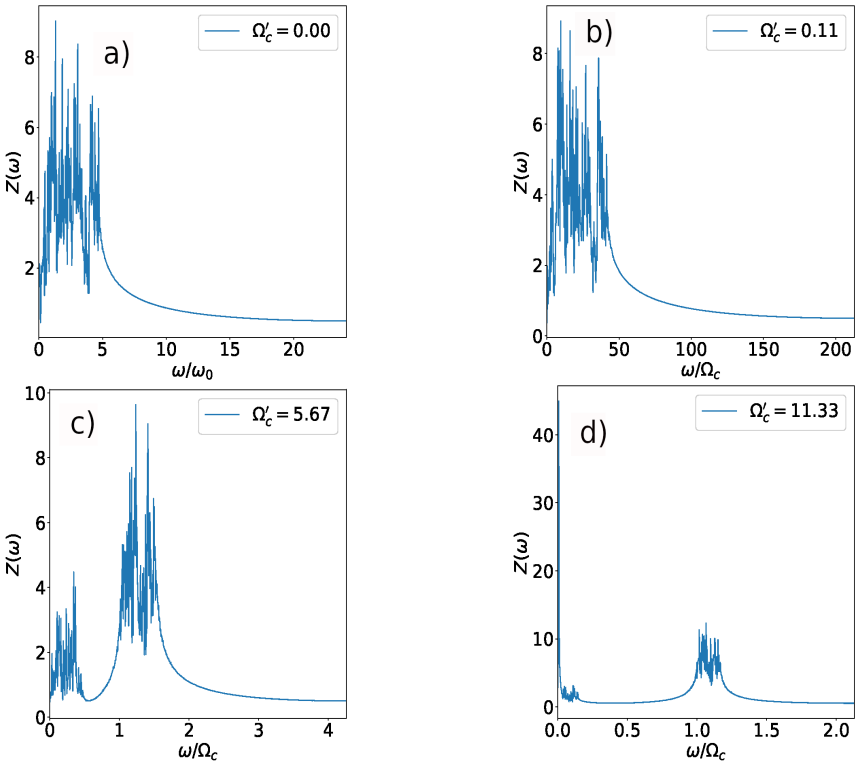

Figure 4.15: The Fourier transformed velocity autocorrelation function is plotted at different values of magnetic field strengths, a) $\Omega_c' = 0.0$, b) $\Omega_c' = 0.11$, c) $\Omega_c' = 5.67$ and d) $\Omega_c' = 11.33$ at $\Gamma = 7274$ and $\kappa = 4.7$.

strength is increased, the phonon states can be seen to be distributed around two distinct frequencies. This trend also resembles the trend observed in the current autocorrelation spectra (Fig. 4.7 and 4.8) where, with the increase of the magnetic field strength the phonon spectra can be seen to be clearly separated into two distinct branches. The density of states function $Z(\omega)$ has some characteristic features corresponding to solid, liquid and gaseous states. In case of gaseous state, $Z(\omega = 0) > 0$ which indicates the presence of diffusive modes at longer timescales and it decays monotonically for $\omega > 0$. For liquid states, $Z(\omega = 0) > 0$ and then $Z(\omega)$ becomes maximum at a certain value of ω and then decays monotonically afterwards. For solid states, $Z(\omega = 0) = 0$ and it goes through a maximum at an intermediate value of ω before decaying monotonically [173]. The plots of $Z(\omega)$ shown in Fig. 4.15 suggest the presence of diffusive modes at longer timescales.

Mean squared displacement

In order to gain further insight into the self-diffusion of particles in the cluster we obtain the mean squared displacement of the cluster of particles. In our simulation the Mean Squared Displacement(MSD) is calculated according to,

$$MSD(t) = \frac{1}{N\tau_{max}} \sum_{\tau=1}^{\tau_{max}} \sum_{j=1}^{N} \Big[\mathbf{r}_j(t+\tau) - \mathbf{r}_j(\tau)\Big]^2, \tag{4.31}$$

where, τ_{max} denotes the maximum number of time origins, t denotes delay time and $\mathbf{r}_j(t)$ denotes the position vector of the jth dust particle at time t.

In general, the MSD as a function of time can be expressed as [174],

$$\Big\langle r^2(t) \Big\rangle = \frac{2dD_\alpha}{\gamma(\alpha+1)} t^\alpha, \tag{4.32}$$

where, d is dimensionality, D_α is diffusion coefficient, α is diffusion exponent and $\gamma(x)$ denotes gamma function. MSD gives idea about the diffusive behaviour of the system of particles. By setting $\alpha = 1$ and $d = 2$ in Eq. 4.32 one can retrieve the scaling law for normal diffusion in a 2D system,

$$\Big\langle r^2(t) \Big\rangle = 4D_1 t. \tag{4.33}$$

In our simulation, MSD is obtained according to Eq. 4.31 and the calculation was repeated for 80 initial conditions before performing ensemble average. MSDs

for a 2D cluster at different magnetic field strengths are shown in Fig. 4.16 at $\Gamma = 7274$ and $\kappa = 4.7$. It is clear from the log-log plot (Fig. 4.16(b)) that the motion of the particles initially remain superdiffusive and the time interval for which it remain superdiffusive reduces as magnetic field strength increases. In the log-log plot the oscillations that are seen at smaller delay times are due to Larmour oscillation of the dust particles. A dip can be seen in the log-log plot of MSD at the time period of cyclotron motion (τ_c) and subsequent dips at integral multiples of τ_c. However, the origin of the oscillations that occur at larger delay times is not immediately obvious. It is seen from Fig. 4.17 that the cluster

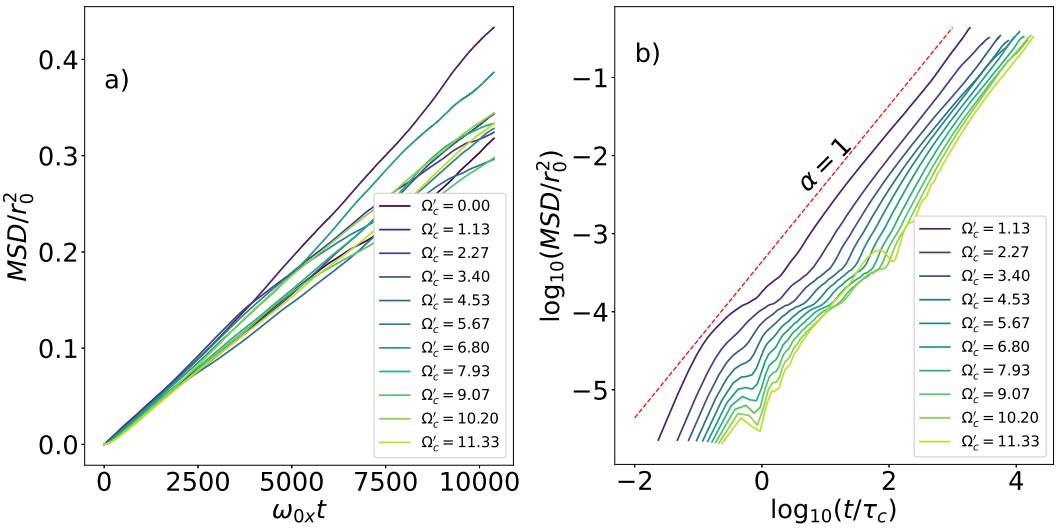

Figure 4.16: a) Mean squared displacement as a function of time at different magnetic field strengths. b) Log-log plot of MSD as a function of time. For both the figures the coupling and screening parameters are fixed as $\Gamma = 7274$ and $\kappa = 4.7$ respectively. The time axis in the log-log plot is scaled by the time period of cyclotron motion $\tau_c = \frac{2\pi}{\Omega_c}$ as indicated.

goes to a superdiffusive regime on increasing the magnetic field strength beyond a certain value. It has been previously observed in bulk 2D dusty plasma that magnetic field leads to superdiffusion [119]. However, it is seen from Fig. 4.17 that the difusion exponents are scattered around the line $\alpha = 1$ upto a certain magnetic field ($\Omega_c' = 5.67$) and then on further increasing the field strength the points lie consistently above $\alpha = 1$. This means that the system shows normal diffusion as the magnetic field strength is increased from zero upto $\Omega_c' = 5.67$ and

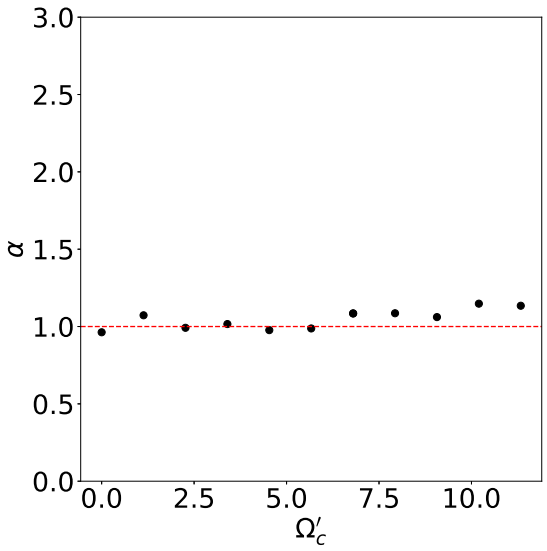

Figure 4.17: Diffusion exponent as a function of magnetic field strength. The values of α are obtained by fitting Eq. 4.32 to the MSD time series for the duration $125.89 < \omega_{0x}t < 10383.23$. The red dashed line is drawn through $\alpha = 1$ to enable the reader compare the values of α in our case to that of normal diffusion. Coupling and screening parameters are fixed as $\Gamma = 7274$ and $\kappa = 4.7$ respectively for these results.

then it becomes superdiffusive. This behaviour is observed due to a competition between two time scales present in our system : the cyclotron time period and the time scale associated with the confinement potential. From Fig. 4.17 it is seen that the crossover from normal diffusion to superdiffusion occurs around $\Omega_c' \sim 6.8$. It is interesting to note that for $\Omega_c' \gtrsim 6.8$ the relation $\tau_c \lesssim \tau_h$ beween cyclotron time period τ_c and harmonic confinement time period τ_h (inverse of confinement frequency) holds true. That is a particle exhibits larmor oscillation before being affected by the harmonic confinement force.

In order to see whether this is a general trend, MSD is obtained also for a lower value of coupling parameter, i.e, $\Gamma = 145.48$. The results are shown in Fig. 4.18.

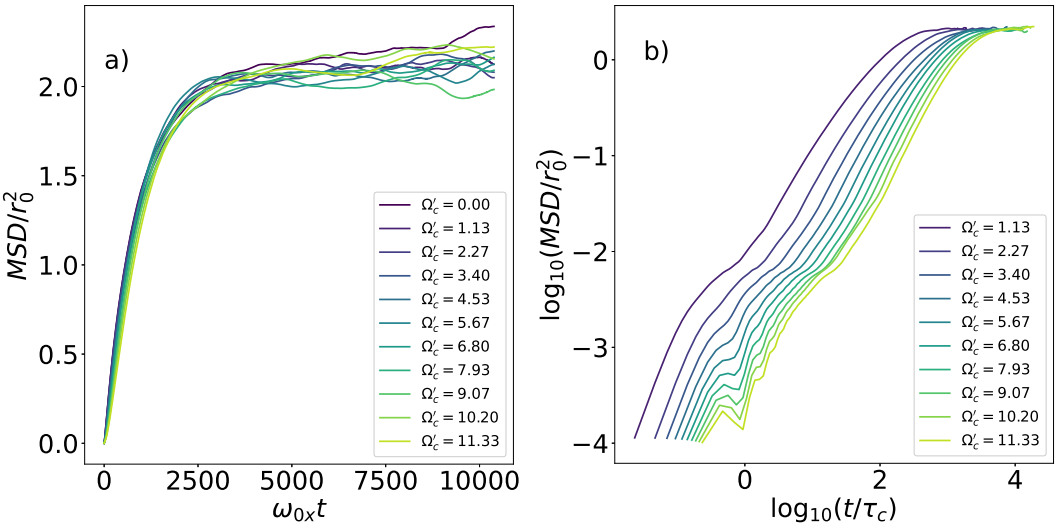

Figure 4.18: a) MSD plotted as a function of time at different magnetic field strengths. b) Log-log plot of MSD as a function of time. For both the figures the coupling and screening parameters are fixed as $\Gamma = 145.48$ and $\kappa = 4.7$ respectively. The time axis in the log-log plot is scaled by the time period of cyclotron motion $\tau_c = \frac{2\pi}{\Omega_c}$ as indicated.

It has been shown that the MSD approaches a value $A_0 = \frac{2k_B T_d}{m\omega_{0x}^2}$ for a delay time $\omega_{0x}t >> 1/\nu'$ when the amplitude of driving continuous oscillations become much smaller than A_0 [175]. For a system with dimensionality d, the equlibrium value of total MSD approaches dA_0. For a harmonically confined cluster of Yukawa inter-

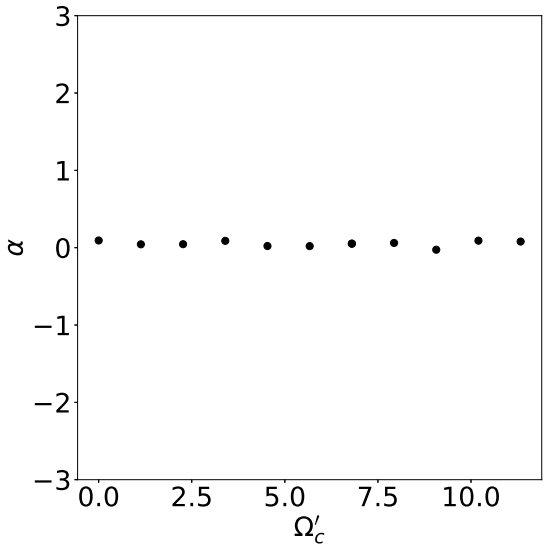

Figure 4.19: Diffusion exponent as a function of magnetic field strength. The values of α are obtained by fitting Eq. 4.32 to the MSD time series for the duration $2511.89 < \omega_{0x}t < 10383.23$. Coupling and screening parameters are fixed as $\Gamma = 145.48$ and $\kappa = 4.7$ respectively for these results.

acting particles, this will happen when, the dust kinetic temperature T_d becomes sufficiently large or equivalently Γ becomes sufficiently small (in our simulation Γ is changed by changing T_d) at a fixed value of confinement strength. In Fig. 4.18(a) this doesn't happen because the dust kinetic temperature corresponding to this figure is much lower ($T_d = 2500\ K$). It can be seen that for the considered duration, the cluster remains subdiffusive at all magnetic field strengths (see Fig. 4.19).

4.5 Summary and Conclusions

In summary, the collective as well as single particle dynamics of 2D Yukawa clusters are investigated as a function of magnetic field strength using Langevin dynamics simulation. The phonon spectra arising due to thermal fluctuations are investigated in the case of a linear dust chain and a 2D dust cluster in the presence of an externally applied perpendicular magnetic field. The spectra are

obtained from the values of Current Autocorrelation Function (CAF) evaluated at different wavenumbers. The particle velocities and positions are sampled from Langevin Dynamics Simulations which can be used to compute CAF and other relevant quantities studied here. The dust particles interacting via the Yukawa potential are confined by harmonic potential which can be applied in laboratory dusty plasma experiments. An analytical model is developed to obtain the dispersion relation of normal modes arising in such systems and the results are found to agree well with that of simulation for the range of parameters studied here. The normal mode of magnetized linear chain is found to consist of two branches. One low frequency acoustic like mode having longitudinal character and the other high frequency optic branch having mixed longitudinal and transverse character. The longitudinal optic branch is characteristic of magnetic field and disappears completely in the absence of magnetic field. The frequency of transverse mode at zero magnetic field decreases with increase in wavenumber and at zero wavenumber the frequency of this mode is attributed to confinement frequency along $y-$direction. The frequency remains almost constant with wavenumbers at larger magnetic field strengths. On the other hand the frequency of the longitudinal acoustic branch is found to increase with wavenumber at all field strengths.

Similar analysis has been performed in 2D dust cluster. The dispersion relation in this case, clearly admits two branches as in a linear chain. Previously, researchers have performed similar analysis in much larger 2D systems both for bulk plasma crystal in the presence or absence of external magnetic field and in harmonically confined system of particles in the absence of external magnetic fields. Zhdanov *et al.* studied the polarization of wave modes in Yukawa monolayer via experiment, simulation and theory and found that the polarization alternates between longitudinal and transverse modes [171]. Farokhi and Shukla did a theoretical normal mode analysis in a 2D bulk plasma crystal in the presence of a perpendicular magnetic field where they observed two branches due to the coupling between the longitudinal and transverse lattice vibrations because of the presence of the Lorentz force [170]. In the present work, the analysis has been performed in a much smaller harmonically trapped system consisting of 34 particles in the presence of an external magnetic field applied perpendicularly. It is observed that

with the increase in the magnetic field strength, the frequency of the upper frequency branch approaches cyclotron frequency. The study further reveals that both longitudinal and transverse modes disappear when damping due to neutral particles approaches cyclotron frequency. It is seen in the present work that when the coupling parameter is large, the system shows normal diffusion at a smaller value of the field strength and then for the higher values of the field strength it becomes superdiffusive. This is contrary to the observation made in the simulation of bulk 2D liquid dusty plasma where the system shows superdiffusion ($\alpha = 1.1$) for stronger magnetic fields and weak superdiffusion ($1 < \alpha < 1.1$) for weaker magnetic fields. [119].

The present analysis shows that several novel features of the phonon spectra emerge both in linear chain and 2D dust cluster once the strength of the transverse magnetic field attains a certain value. Combined action of Yukawa interaction, harmonic confinement as well as the Lorentz force brings out new normal modes of such system. Strong magnetic field is manifested as splitting of energy associated with the modes for particular wavenumber into two states. In the present system, the nature of the normal modes are controlled by four different time scales i.e, the collision time scale, harmonic time scale, the cyclotron time scale and the time scale associated with interaction among dust grains. It is the competition among these time scales that gives rise to the interesting collective and single particle dynamics reported here. The magnetized phonon spectra studied in this paper can be realized in strongly coupled dusty plasma in the presence of a magnetic field such that the cyclotron time scale (τ_c) is comparable to the interaction time scale (τ_{int}).